

RESEARCH ARTICLE



Effect of Huangqin decoction on regulating intestinal flora in colitis mice characterized as inhibition of the NOD2-dependent pathway

Shaowei Huang^a, Jinrong He^a, Yanping Chen^a, Xiaojing Wang^a, Yanyang Li^a, Yulin Su^a, Ruyan Wen^b, Xiuling Li^c, Guanghua Yang^a, Shuang Luo^a, Lian Zhou^a and Xia Luo^a

^aSchool of Pharmaceutical Sciences, Guangzhou University of Chinese Medicine, Guangzhou, China; ^bInstitute: Guangxi Scientific Experimental Center of Traditional Chinese Medicine, Guangxi University of Chinese Medicine, Nanning, China; ^cSun Yat-sen University, Guangzhou, China

ABSTRACT

Context: Chinese herb Huangqin decoction (HQD) can regulate intestinal flora in ulcerative colitis (UC) mice.

Objective: Our study clarifies the mechanism of HQD in regulating the intestinal flora of UC mice.

Materials and methods: Male C57BL/6 mice were randomly divided into six groups: Control, Model (3% DSS), Sulfasalazine (500 mg/kg), HQD-L (250 mg/kg), HQD-M (500 mg/kg), and HQD-H (1000 mg/kg) groups. Measurement of body weight, colon length, DAI, and haematoxylin–eosin staining were conducted. FISH and 16S rDNA detected colonic bacterial infiltration and intestinal flora changes. The expression of RegIII γ and PRRs (NOD2, TLR5, TLR4) were detected by FCM and WB, respectively. In addition, WB, qPCR, or IHC were used to detect the expression of NOD2, MyD88, RIP2, and NF- κ B p65 in the colon. ELISA was used to determine cytokines.

Results: Compared with the model group (DAI score, 2.38 ± 0.05 ; histological score, 4.08 ± 0.54), HQD treatment significantly reduced the DAI score (L, 2.16 ± 0.09 ; M, 1.45 ± 0.05 ; H, 1.18 ± 0.05) and histological score (L, 3.16 ± 0.82 ; M, 2.50 ± 0.81 ; H, 1.51 ± 0.76); restored the weight, the colonic length ($p < 0.05$). 16S rDNA identification showed HQD regulated the balance of intestinal flora. Moreover, HQD suppressed the expression of RegIII γ ($p < 0.05$) and prevented colonic bacterial infiltration. Furthermore, WB results showed NOD2, and TLR4 were inhibited by HQD, especially NOD2 ($p < 0.01$). The data of WB, qPCR, and IHC demonstrated that the NOD2-dependent pathway was inhibited by HQD ($p < 0.01$).

Discussion and conclusions: HQD (1000 mg/kg) regulates the intestinal flora of colitis mice, mainly characterized as inhibition of the NOD2-dependent pathway. These results indicate that HQD has potential.

ARTICLE HISTORY

Received 14 April 2021
Accepted 8 December 2021

KEYWORDS

Ulcerative colitis; nucleotide binding oligomerization domain containing 2; HQD; muramyl dipeptide; NF- κ B

Introduction

Ulcerative colitis (UC), a chronic inflammatory bowel disease (IBD) characterized by recurrent episodes of intestinal inflammation, is challenging to cure because of its complicated etiology (Ungaro et al. 2017). Accumulating research shows that the occurrence and development of UC are strongly associated with the disorder of intestinal flora (Weingarden and Vaughn 2017; Nishida et al. 2018). Intestinal symbiotic bacteria form a microbial barrier in physiological states, which can resist the invasion of pathogenic bacteria (Zhang et al. 2017). However, the microbial barrier is damaged due to the imbalance of intestinal flora. The microbes and their metabolites invade the intestinal epithelial cells, causing inflammation and even apoptosis and destroying the intestinal physiological function. What is more, the abundance of probiotics such as *Bifidobacterium* and *Lactobacillus* in UC decreases significantly, while the pathogenic bacteria such as *Escherichia coli* increase significantly (Zhang and Shen 2018). Therefore, regulating the balance of intestinal flora plays an essential role in the treatment of UC.

It is reported that pathogen-associated molecular patterns (PAMPs), mainly derived from intestinal bacteria, excessively trigger the immune system, releasing pro-inflammatory cytokines and further destroying the intestinal barrier (Geremia et al. 2014; Wang et al. 2019). PAMPs, like lipopolysaccharides (LPS), flagellin, muramyl dipeptide (MDP), are recognized by pattern recognition receptors (PRRs), which activates PRRs (LPS combined with TLR4, flagellin combined with TLR5, and MDP combined with NOD2) and their downstream signalling pathways to release inflammatory cytokines, recruit phagocytic cells, and regulate dendritic cells. In a study of PRRs, the nucleotide-binding oligomerization domain-containing protein 2 (NOD2)-dependent pathway is found to be influential among multiple inflammatory signalling pathways, and *Nod2* is the first susceptible gene found to be associated with IBD (Germain et al. 2016). The number of bacteria adhering to the intestinal mucosa increased in UC patients with NOD2 gene mutation. In addition, some studies also indicate that the expression of Toll-like receptor (TLR) 4 and TLR5 increased in UC mice (Luo et al. 2018; Wang et al. 2019).

CONTACT Lian Zhou ✉ zl@gzucm.edu.cn 📍 Room B318, Pharmaceutical Building, Guangzhou University of Chinese Medicine, No. 232 Outer Ring Road, Panyu District, Guangzhou City 510006, China; Xia Luo ✉ luoxia@gzucm.edu.cn 📍 Room B318, Pharmaceutical Building, Guangzhou University of Chinese Medicine, No. 232 Outer Ring Road, Panyu District, Guangzhou City 510006, China

© 2021 The Author(s). Published by Informa UK Limited, trading as Taylor & Francis Group.

This is an Open Access article distributed under the terms of the Creative Commons Attribution-NonCommercial License (<http://creativecommons.org/licenses/by-nc/4.0/>), which permits unrestricted non-commercial use, distribution, and reproduction in any medium, provided the original work is properly cited.

Accumulating evidence shows that Huangqin decoction (HQD), a well-known traditional Chinese herbal prescription documented in the book *Treatise on Febrile Diseases* from the Han dynasty, prevents intestinal carbuncles such as UC. Nowadays, the prescription is widely used in the clinical treatment of UC (Xi 2006; Ning et al. 2014), and its mechanism is mainly related to the maintenance of intestinal epithelial cell homeostasis, protection of intestinal barrier (Zou et al. 2016), inhibition of TLR4/MyD88 signal pathway (Wang et al. 2016), suppression of immune response, regulation of intestinal flora (Yang et al. 2017; Wan 2020). However, the effect of HQD on the relation of intestinal PRRs and intestinal flora in patients with colitis is unclear. Thus, our study uses DSS-induced colitis mice as a model of UC to explore the regulation of HQD on the intestinal flora and PRRs.

Materials and methods

Drugs and reagents

HQD consists of the following component herbs: the root of *Paeonia lactiflora* Pall. (Ranunculaceae), the root of *Glycyrrhiza uralensis* Fisch. (Leguminosae), the fructus of *Ziziphus jujuba* Mill. (Rhamnaceae) (purchased from Kangmei Pharmaceutical Co., Ltd., Puning, China), and the root of *Scutellaria baicalensis* Georgi (Lamiaceae) (purchased from Guangdong He Xiang Pharmaceutical Co., Ltd., Guangdong, China). Paeoniflorin and baicalin were purchased from Guangzhou Whiga Technology Co., Ltd. (Guangzhou, China). Liquiritin ($\geq 98\%$ purity), glycyrrhizic acid ($\geq 98\%$ purity), and wogonoside ($\geq 98\%$ purity) were purchased from Chengdu Feipude Biological Technology Co., Ltd. (Chengdu, China). The cytometric bead array (CBA) assay kit was purchased from BD Biosciences Pharmingen (San Jose, CA). DSS was obtained from MP Biomedicals (Santa Ana, CA). Sulfasalazine tablets were purchased from Shanxi Tongda Pharmaceutical Co., Ltd. (Shanxi, China). The TRIZol reagent, NF- κ B p65 gene primers, and receptor-interacting protein-2 (RIP2) gene primers were purchased from Invitrogen (Carlsbad, CA). SYBR®Premix Ex Taq™ (TliRNaseH Plus), DNase/RNase-free deionized water, NOD2 gene primers, and glyceraldehyde 3-phosphate dehydrogenase (GAPDH) reference gene primers were obtained from Dalian Bioengineering Co., Ltd. (Dalian, China). The anti-TLR4 antibody, anti-MyD88 antibody, anti-RIP2 antibody, and anti-NF- κ B p65 antibody were purchased from Cell Signaling Technology (Boston, MA). An anti-NOD2 antibody was purchased from Abcam (Cambs, UK). Protein markers were purchased from Fermentas (Burlington, ON, Canada). The enhanced chemiluminescence (ECL) substrate was purchased from the Beyotime Institute of Biotechnology (Shanghai, China).

Preparation of HQD

According to the original proportion (9: 6: 6: 6, g), we weighed and mixed *S. baicalensis*, *P. lactiflora*, *G. uralensis*, and *Z. jujuba* and prepared 10 batches of a traditional decoction. Each was mixed with eight times the amount of water, soaked for 30 min, then subjected twice to the first fire to boil for 25 min and simmer for about 35 min, and filtered. The two filtrates were combined and subjected to rotary evaporation to obtain a solution equivalent to 2 g/mL crude drug. The solution was diluted with ultrapure water to 0.5 g/mL and further diluted with an equal volume of methanol to a final concentration of 0.25 g/mL. A test

sample was obtained after centrifugation for 1 min and filtration through a 0.22 μ m membrane.

Baicalin, paeoniflorin, glycyrrhizin, and glycyrrhizic acid (5 mg each) were dissolved in 10 mL of methanol and filtered through a 0.45 μ m microporous membrane. Paeoniflorin was diluted to a final concentration of 40 μ g/mL with 50% methanol, and the other reference substances were diluted to 20 μ g/mL. All compounds were prepared as a single standard and mixed standard, followed by centrifugation for 1 min and filtration through a 0.22 μ m membrane.

The prepared HQD and reference substance solutions were analyzed by high-performance liquid chromatography (HPLC). The results of an HPLC chromatogram were imported into software (Chinese medicine chromatographic fingerprint similarity evaluation system 2004 A) to analyze its fingerprint in an Analytical Instrument Association (AIA) format. The fingerprint of HQD sample S1 was used as a reference spectrum, and control maps were generated using average data. Fingerprint matching was performed by a multi-point calibration method to generate a control map. The following chromatographic conditions were used: a Kromasil C18 column (250 mm \times 4.6 mm, 5 m); column temperature: 30 °C; mobile phase A: acetonitrile; mobile phase B: water containing 0.1% phosphoric acid; linear elution gradient: 0–10 min, 10–11% A; 10–35 min, 11–65% A; flow rate: 1.0 mL/min; scanning wavelengths: 220–500 nm; sample size: 10 μ L.

Animals

C57BL/6 mice (male, 6–8-week-old, weight 18–22 g) were obtained from the Laboratory Animal Center of Guangzhou University of Chinese Medicine (Guangzhou, China) and acclimated for at least 3 days before experiments. The mice were housed in groups under specific pathogen-free conditions at a temperature of 24 \pm 1 °C, 40–80% humidity, and a 12 h light/dark cycle. All experiments were executed according to the guidelines approved by the Ethics Committee of Guangzhou University of Chinese Medicine.

Induction of colitis and treatments

C57BL/6 mice were randomly divided into six groups ($n = 12$ per group): control, model (DSS), sulfasalazine (500 mg/kg), low dose of HQD (250 mg/kg), medium dose of HQD (500 mg/kg), and high dose of HQD (1000 mg/kg) groups. The mice in the control group had free access to sterile water, while those in the other groups drank 3% DSS freely for 5 days and then drank sterile water. Meanwhile, the mice in the control and model groups were administered sterile water, while the other four were given complementary medicines. The drugs were administered for 10 days according to the mouse weight (0.2 mL/10 g), and the experiment was carried out on day 11. The grouping and treatment with HQD of the DSS-induced colitis mice are shown in Figure 1.

Assessment of colitis severity

The disease activity index (DAI) score of colitis was determined as Cooper previously described (Cooper et al. 1993). To assess the severity of colitis in mice, eating, water drinking, the hair colour, faeces, blood in the stool, and the body weight were carefully observed and recorded daily.

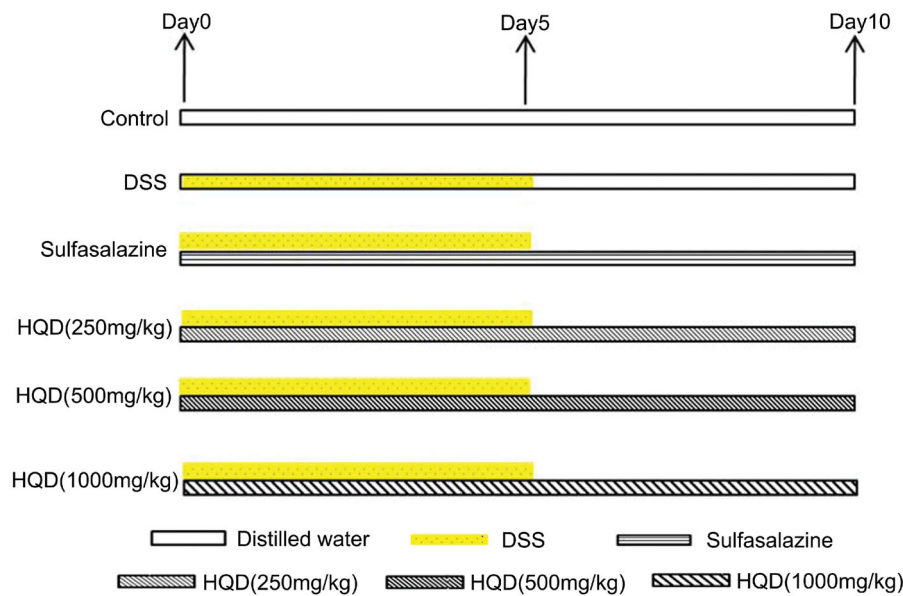


Figure 1. Treatment of HQD on colitis mice induced by DSS. The mice in the control group had free access to sterile water, while those in the other groups drank 3% DSS freely for 5 days and then drank sterile water. Meanwhile, the mice in the control and model groups were administered sterile water, while the other four groups were given the drugs. The drugs were administered for 10 days, and the experiment was carried out on day 11.

Table 1. Criteria for histological grading.

Score	Injury of colonic tissue
0	No ulcer, no inflammation
1	Local mucosal hyperaemia, no ulcer
2	Formation of ulcer
3	Single ulcer, mucosal inflammation
4	Multiple ulcers, mucosal inflammation
5	Ulcer area > 2 cm, mucosal hyperaemia, edoema and severe erosion

At the end of the administration, peripheral blood was collected from the eyes after anaesthesia, then 20 μ L was thoroughly mixed in an EDTA-2K anticoagulant tube and used to count blood cells with an automatic blood cell analyzer. Then, mice were sacrificed by cervical dislocation. We cut colonic segments from the sacrificed mice and recorded their natural length without stretching. The distal colon of 2.0 cm was fixed with 4% paraformaldehyde, dehydrated, and embedded in paraffin. The tissue was cut into about 4 μ m slices and stained with haematoxylin and eosin (HE). Then, the stained tissue was observed under an optical microscope, and a histological score was determined according to the standard shown in Table 1.

16s ribosomal DNA (16S rDNA) identification

The caecum contents were taken aseptically and were detected by Shenzhen Huada Genomics Technology Service Co., Ltd. (Shenzhen City, China) using 16S rDNA sequencing technology.

Cytokine detection by cytometric bead array (CBA) and flow cytometry (FCM)

A colonic segment was mixed with 0.9% NaCl saline at a mass ratio of 1:10 and then automatically homogenized with a homogenizer. The homogenate was centrifuged to obtain a supernatant (3000 \times g, 4 $^{\circ}$ C, 10 min). The levels of interleukin (IL)-1 β , IL-17, IL-6, monocyte chemotactic protein-1 (MCP-1), TNF- α ,

and interferon- γ (IFN- γ) were determined by CBA following the manufacturer's instructions using a FACS CantoII flow cytometer.

IECs were extracted from the small intestine with digestive juice and incubated with Alexa Fluor 488-CD324, and PE-RegIII γ flow antibody for 30 min. Intestinal epithelial cells were labelled with CD324 and antibacterial proteins were labelled with RegIII γ . Then, they were detected by flow cytometry.

Fluorescence in situ hybridization (FISH)

Four micrometre sections were prepared from paraffin-embedded colon tissue for FISH. According to the manufacturer's instructions, bacterial infiltration of the colonic mucosa was detected using the EUB338I FISH probe with FITC-labelled kit (Guangzhou Exon Biotechnology Co., Ltd., Guangzhou, China).

Western blot analysis

Colonic tissue was homogenized and centrifuged (4 $^{\circ}$ C, 2500 \times g, and 5 min). Cytoplasmic and nuclear proteins were extracted from the collected precipitate using cytoplasmic and nuclear protein extraction kits, respectively. The protein concentration was calculated by measuring optical density at 562 nm with a microplate reader. Proteins (20 μ g) were separated by sodium dodecyl sulfate-polyacrylamide gel electrophoresis and then transferred onto a polyvinylidene difluoride membrane. The membrane was soaked in 5% skim milk at room temperature for 1 h to block non-specific binding sites and then incubated with a primary antibody (TLR4, TLR5, NOD2, MyD88, RIP2, or NF- κ B p65), followed by incubation with an appropriate secondary antibody. Positive immunoreactions were directly imaged using a chemiluminescence image analysis system with a Super ECL Plus ultra-sensitive luminescent solution.

Semi-quantitative reverse transcription and polymerase chain reaction

Total RNA was extracted from the colon with the TRIzol reagent. The purity and the concentration of RNA were determined using an ultra-micro ultraviolet spectrophotometer, and the concentration was adjusted to 500–700 ng/ μ L. DNA was removed from the total RNA using DNase with incubation at 42 °C for 5 min. cDNA was synthesized from 1 μ g of total RNA in a total volume of 20 μ L at the following conditions: 37 °C for 15 min, followed by 85 °C for 5 s with a first-strand cDNA synthesis kit. SYBR®Premix Ex Taq™ (TliRNaseH Plus) was used for amplification of cDNA. Reactions were performed in triplicate. We analyzed the relative expression of the *Nod2*, *Rip2*, and *NF- κ Bp65* genes by comparing transcript levels of the target genes with that of the internal reference *Gapdh*. The sequences of the primers were as follows: *Nod2*: 5'-ACCATGTAGAAGCCATGCTGGAG-3' (forward) and 5'-CTTCAACCGCAGC GAGATCAA-3' (reverse); *Rip2*: 5'-GCCATTGTGAGCCAGATGA-3' (forward) and 5'-ATTTGAAGGCGGTGCTTTG-3' (reverse); *RelA* (encoding *NF- κ Bp65*): 5'-ATGTGCATCGGCAAGTGG-3' (forward) and 5'-CAGAAGTTGAGTTTCGGTAG-3' (reverse); *Gapdh*: 5'-ACCACAGTCCATGCCATCAG-3' (forward) and 5'-TCCACCACCCTGTTGCTGTA-3' (reverse). The amplification conditions were as follows: 95 °C for 30 s, 40 cycles at 95 °C for 5 s and 60 °C for 30 s, followed by 95 °C for 10 s and generation of a dissociation curve from 65 °C to 95 °C at an increment of 0.5 °C per 5 s.

Immunohistochemistry analysis

Antigens were retrieved from frozen sections with citrate buffer, and the sections were then fixed with acetone and washed with phosphate-buffered saline. After that, H₂O₂ (20 μ L/sample) was added to inhibit the endogenous enzyme, followed by a blocking solution. The sections were exposed to anti-NOD2, anti-RIP2, or anti-NF- κ B p65 at 4 °C overnight and then to the SignalStain®

Boost IHC detection reagent at room temperature for 30 min. Images were visualized and captured using an Olympus microscope after staining with haematoxylin, dehydration, and sealing.

Statistical analysis

Data are expressed as the mean \pm standard deviation (SD). Student's *t*-test analyzed differences between the two groups, and those among several groups were analyzed by one-way analysis of variance using SPSS (version 17.0, SPSS Inc., Chicago, IL). A *p*-value of <0.05 was considered statistically significant.

Results

HPLC analysis of HQD

It has been reported that HQD was confirmed to contain the indicator components paeoniflorin, glycyrrhizic acid, baicalin, wogonoside, and liquiritin, among which baicalin had the highest concentration, followed by wogonoside and glycyrrhizic acid (Huang et al. 2020). And our results showed that the sample similarity of the 10 batches of HQD was more than 0.980, based on the HQD fingerprints (Figure 2), and the similarity analysis (Table 2) indicated that the quality of HQD was relatively stable.

Table 2. Similarity of ten batches of Huangqin decoction.

Sample	Similarity
Hungaqin Decoction S1	0.999
Hungaqin Decoction S2	0.999
Hungaqin Decoction S3	0.999
Hungaqin Decoction S4	0.998
Hungaqin Decoction S5	0.999
Hungaqin Decoction S6	0.998
Hungaqin Decoction S7	1.000
Hungaqin Decoction S8	1.000
Hungaqin Decoction S9	1.000
Hungaqin Decoction S10	0.998

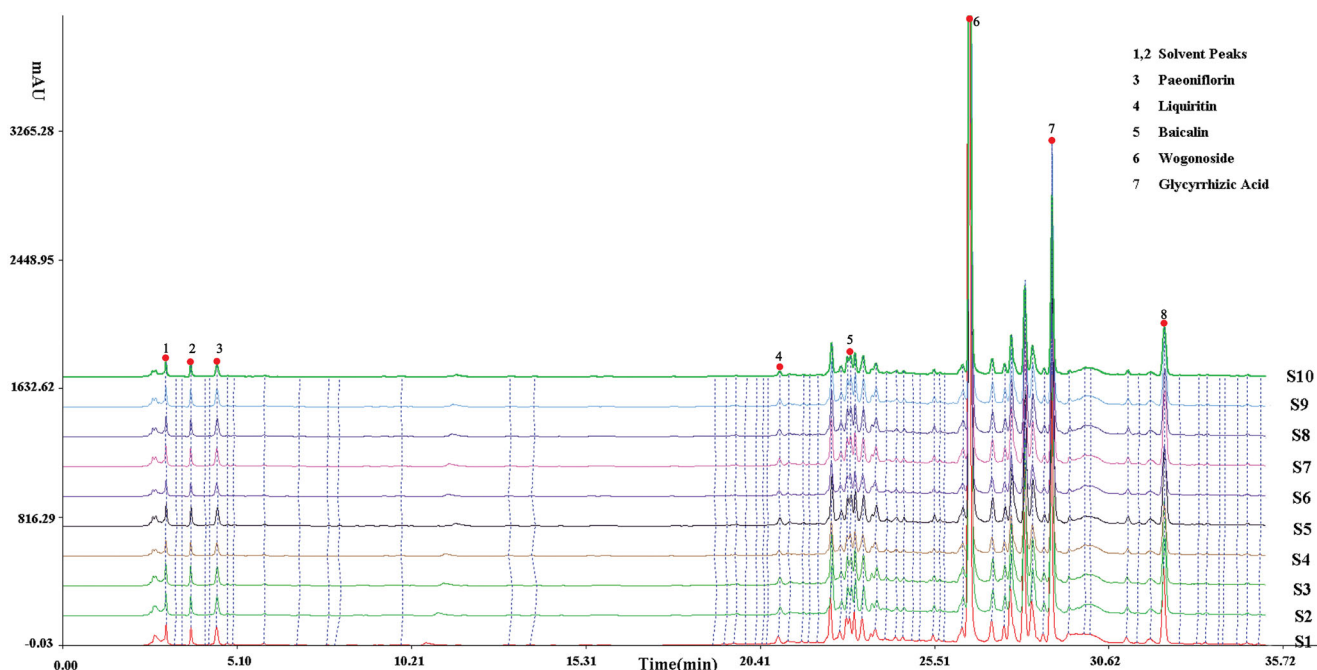


Figure 2. Composition of HQD. Fingerprints of HQD from 10 batches. The sample similarity of the HQD batches was more than 0.980, which proved that the quality of HQD was stable. (1,2) Solvent peaks; (3) Paeoniflorin; (4) Liquiritin; (5) Baicalin; (6) Wogonoside; (7) Glycyrrhizic acid.

Effects of HQD on colitis mice

The experiments showed that the body weight of the mice significantly decreased in the model group (15.78 ± 2.1 g) compared with that of the control group (20.9 ± 0.6 g), sulfasalazine group (20.18 ± 0.66 g), middle-dose (500 mg/kg, 18.91 ± 0.61 g), and high-dose (1000 mg/kg, 19.68 ± 0.51) HQD group. Notably, the body weight of the high-dose HQD group was closed to that of the control mice at the end of administration (Figure 3(a)). The DAI score in the middle-dose and high-dose HQD groups significantly decreased ($p < 0.01$), whereas low-dose HQD exerted negligible influence (Figure 3(c)). While assessing the length of the colon, HQD also showed specific effects on the recovery of colonic length compared with that of the model group ($p < 0.01$, Figure 3(b)).

Based upon the results of HE staining (Figure 3(d)), it was found that the colon in the model group showed apparent inflammatory cell infiltration and formed multiple ulcers ($p < 0.01$). Likewise, HQD provided a therapeutic effect ($p < 0.05$ or $p < 0.01$) in a dose-dependent manner. Comparing with those in the control group, the counts of WBC, monocytes, and granulocytes significantly increased in the model group; however, the counts of red blood cells (RBC) and the levels of haemoglobin (HGB) showed opposite trends ($p < 0.01$). HQD and SASP improved the symptoms observed in the model group ($p < 0.01$ or $p < 0.05$; Figure 3(e)).

Effects of HQD on intestinal flora

Compared with the control group (592.67 ± 32.09), OTU in the DSS group (489.33 ± 65.66) decreased significantly, which were

reversed after intervention with HQD (1000 mg/kg, 562.83 ± 33.46 , Figure 4(a)). Moreover, the results of cluster analysis showed that HQD improved the imbalance of intestinal flora in mice with colitis and tended to the normal level (Figure 4(b,c)). According to the results of α diversity analysis, observed species index, Chao index, ace index, and Shannon index of intestinal flora decreased ($p < 0.05$), while Simpson index increased significantly after DSS administration. Observed species index, Chao index, and ace index were recovered after treatment with HQD, with a significant difference compared with the model group (Figure 4(d)).

In addition, the phylum classification of intestinal flora species showed that *Bacteroidetes* decreased, while *Deferribacteres* and *Firmicutes* increased significantly in colitis mice (Figure 4(e)). Moreover, *Actinobacteria*, *Bacteroidetes*, and *Epsilon-proteobacteria* decreased, and *Bacilli*, *Betaproteobacteria*, *Clostridia*, *Deferribacteres* increased significantly at the class level in colitis mice (Figure 4(e)). SASP and HQD reduced the abundance of *Deferribacteres* at the phylum and class level. In addition, the family classification showed that *Helicobacteraceae*, *S24-7* decreased, while *Alcaligenaceae*, *Anaplasmatocaceae*, *Bifidobacteriaceae*, *Deferribacteraceae*, *Lachnospiraceae*, and *Ruminococcaceae* increased significantly in colitis mice (Figure 4(e)). SASP and HQD decreased the abundance of *Alcaligenaceae* and *Deferribacteraceae* at the family level (Figure 4(f)).

Effects of HQD on intestinal barrier and PRRs

As shown in Figure 5(a), the colonic mucosal bacterial infiltration was more severe in the 3% DSS group than the control

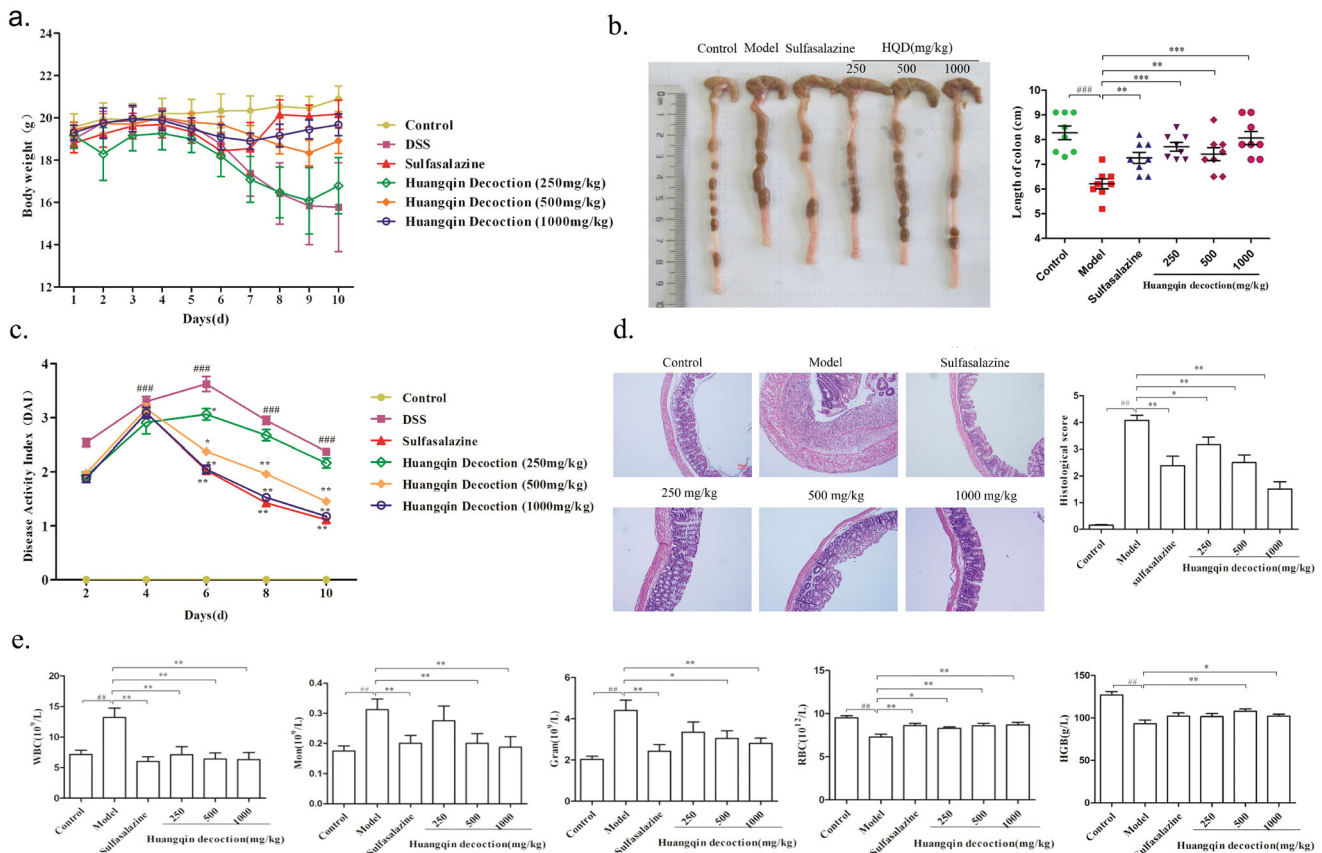


Figure 3. Effect of HQD on colitis mice. (a) Effects of HQD on the body weight of colitis mice. (b) Effects of HQD on the length of the colon in DSS-induced colitis mice ($n = 8$ per group). (c) Effects of HQD on the DAI score of DSS-induced colitis mice ($n = 8$ per group). (d) Effects of HQD on the colon in DSS-induced colitis mice. Scale bar: 50 μ m. (e) Effects of HQD on blood cells in DSS-induced colitis mice ($n = 10$ per group). HQD and sulfasalazine improved the symptoms in the model group. * $p < 0.01$, ** $p < 0.001$ versus DSS-treated group; # $p < 0.05$, ## $p < 0.01$ model versus control.

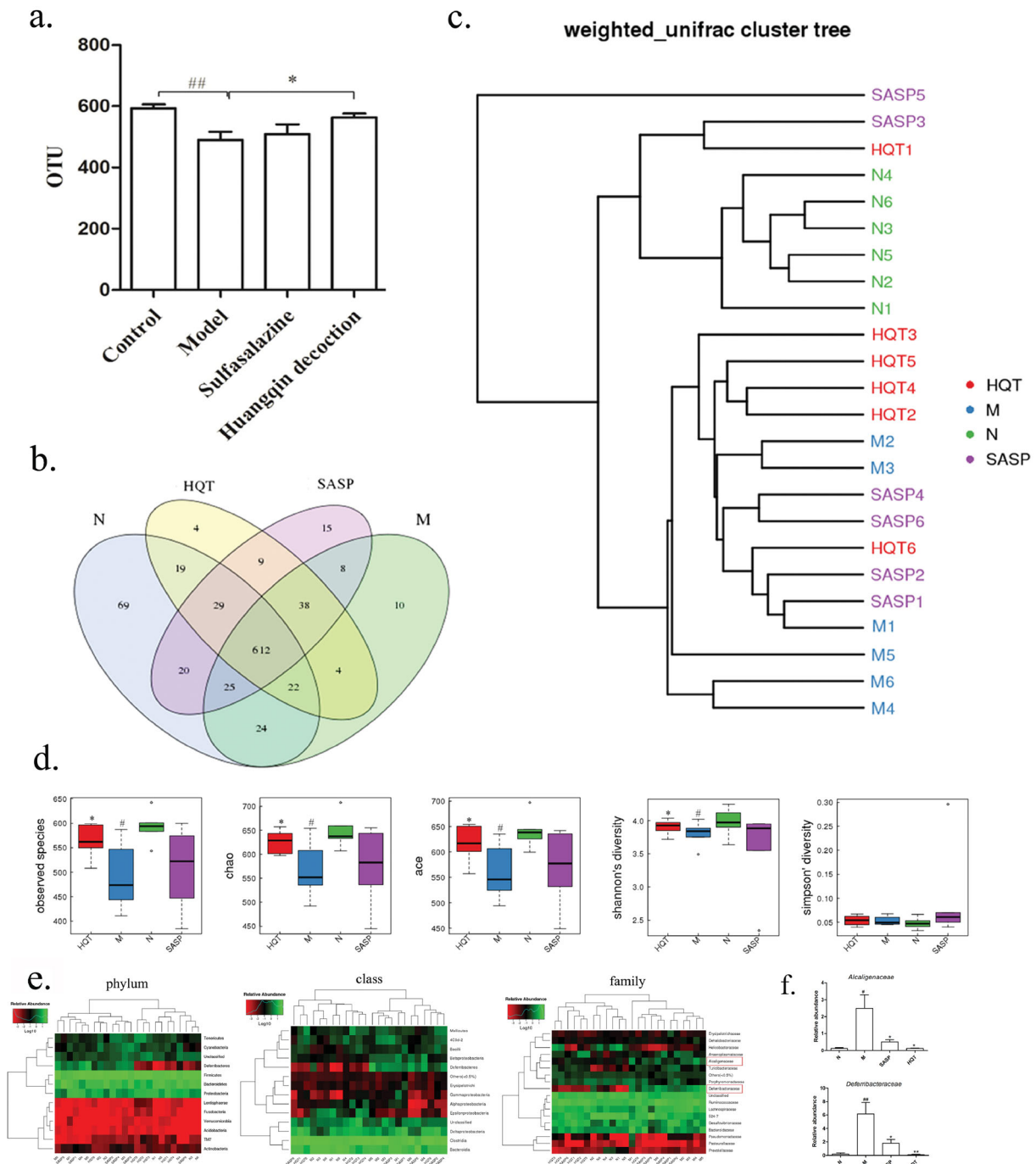


Figure 4. Effect of HQD on intestinal flora of colitis mice. (a) Impacts of HQD on the OTUs of intestinal microflora. (b and c) The cluster analysis of intestinal microflora in colitis mice. (d) The alpha diversity of intestinal microflora in colitis mice. (e) The histogram of intestinal microflora species classification in phylum, class, and family in colitis mice. (f) Impacts of HQD on the abundance of *Alcaligenaceae* and *Deferrbacteraceae* at the family level. N: Control; M: Model; HQT: Huangqin decoction; SASP: sulfasalazine. # $p < 0.05$, ## $p < 0.01$ control versus DSS-treated group, * $p < 0.05$, ** $p < 0.01$ versus DSS-treated group.

group and was reduced after the administration of HQD (1000 mg/kg) and SASP. Compared with the control group (41.96 ± 9.08), the expression of RegIII γ in IECs in the 3% DSS group (63.50 ± 13.04) increased significantly, which were ameliorated with HQD (49.06 ± 9.77) or SASP (48.85 ± 10.32 , Figure 5(b)). What is more, HQD inhibited the increase of TLR4 ($p < 0.05$) and NOD2 ($p < 0.01$) protein in the colon of colitis mice, especially NOD2 (Figure 5(c,d)). Nevertheless, the expression of TLR5 protein in the HQD group was not significantly changed compared with the model group. Furthermore, western blot analysis showed that HQD

(1000 mg/kg) had no significant effect on the downstream pathway protein MyD88 of TLR4 or TLR5, but it inhibited the activation of protein RIP2 in the downstream pathway of NOD2 ($p < 0.05$, Figure 6(a)).

Effects of HQD on NOD2-dependent pathway

NOD2, RIP2, and NF- κ B p65 are the critical proteins in the NOD2 inflammatory signalling pathway. It was demonstrated by a semi-quantitative polymerase chain reaction and

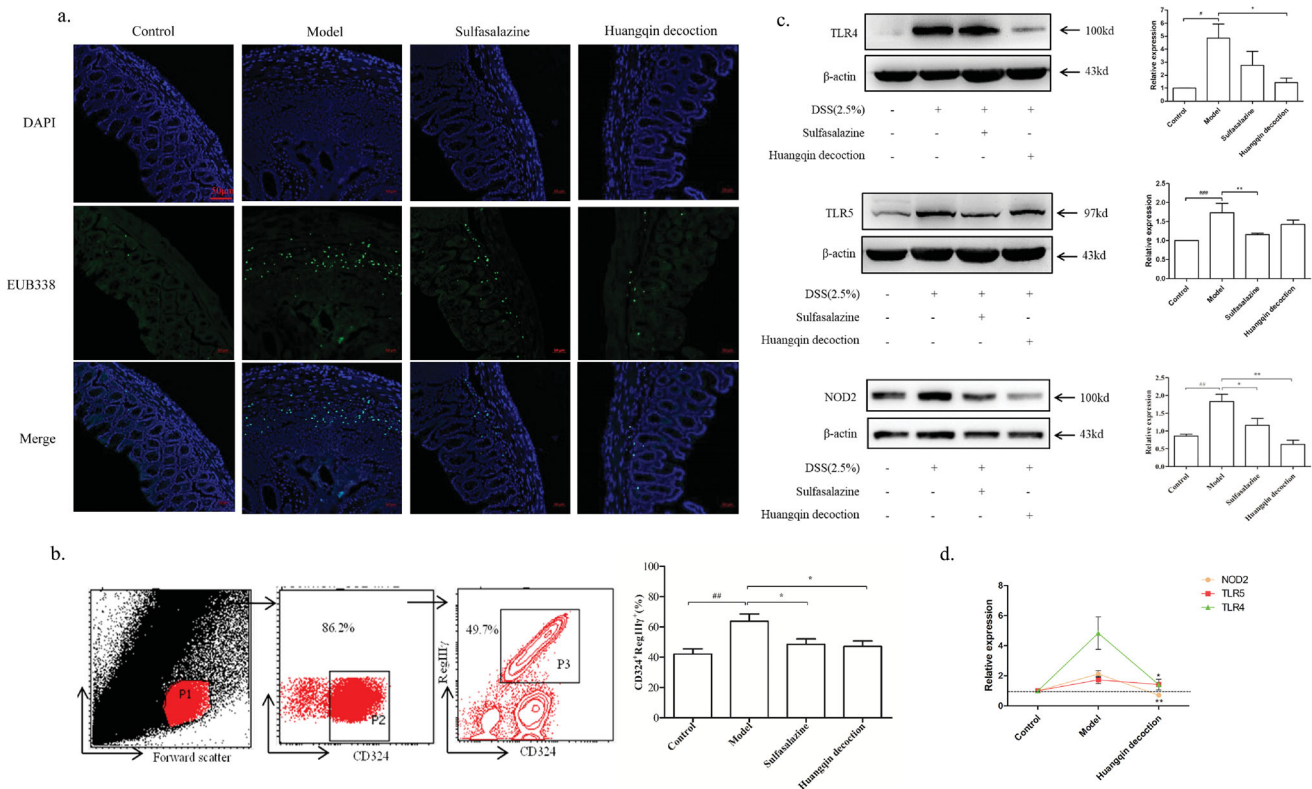


Figure 5. Effect of HQD on PRRs and intestinal barrier function of colitis mice. (a) Impact of HQD on the bacterial submucosal invasion in colitis mice by FISH. Bacteria labelled with green-fluorescence, the cell nucleus labelled with DAPI (magnification $\times 200$). Scale bar: 50 μm . (b) Impacts of HQD on the RegIII γ in IECs by FCM. The analytical protocol of IECs expressed RegIII γ and the statistical results of CD324⁺RegIII γ ⁺ IECs mice. (c) Impacts of HQD on PRRs (TLR4, TLR5, NOD2) in colitis mice by western blot. Quantification of protein expression was performed by densitometric analysis of western blots. Expression was normalized to that of β -actin. Data are expressed as the means \pm SD of three independent experiments. (d) Comparison of HQD on the expression of three PRRs (TLR4, TLR5, NOD2) proteins. $\#p < 0.05$, $\#\#p < 0.01$, $\#\#\#p < 0.001$ control versus model, $*p < 0.05$, $**p < 0.01$ versus model.

immunohistochemistry (IHC) that the colons from the control mice had low levels of NOD2, RIP2, and NF- κ B p65 expression, whereas the mice from the model group with DSS-induced colitis mainly showed overexpression of NOD2, RIP2, and NF- κ B p65 in inflamed colon tissues ($p < 0.01$; Figure 6(b,c)). In the SASP and HQD-treated groups, the expression of NOD2, RIP2, and NF- κ B p65 decreased, especially in the middle-dose and high-dose HQD groups ($p < 0.01$ or $p < 0.05$).

Effects of HQD on inflammatory cytokines

The levels of inflammatory cytokines, including IL-1 β (Figure 7(a)), IL-17 (Figure 7(b)), MCP-1 (Figure 7(c)), TNF- α (Figure 7(d)), IFN- γ (Figure 7(e)), and IL-6 (Figure 7(f)), were significantly higher in colon tissue of the mice from the model group (IL-1 β , 5.10 ± 1.45 ; IL-17, 229.99 ± 29.86 ; MCP-1, 11.36 ± 3.31 ; TNF- α , 728 ± 441.37 ; IFN- γ , 38.63 ± 18.01 ; IL-6, 381.64 ± 96.73) than in that of the control group (IL-1 β , 3.47 ± 0.72 ; IL-17, 1.76 ± 0.74 ; MCP-1, 2.95 ± 0.13 ; TNF- α , 5.56 ± 2.87 ; IFN- γ , 1.2 ± 0.65 ; IL-6, 11.10 ± 6.89 ; $p < 0.01$), and TNF- α was found at the highest level. Compared with the model group, the above markers were restored to varying degrees in the groups treated with different doses of HQD and SASP, especially the medium-dose and high-dose HQD groups ($p < 0.01$ or $p < 0.05$).

Discussion

In this study, we investigated the Chinese medicine compound HQD's potential effect on the intestinal flora of colitis mice and

attempted to clarify the underlying molecular mechanisms in detail. First, the quality of HQD we detected was relatively stable, providing a basis for studying its pharmacodynamics and pharmacological mechanism, which was consistent with what has been previously reported (Li et al. 2019). We proceeded to use a mouse model of DSS-induced colitis, a well-established experimental model with signs and symptoms similar to those observed in human UC, to estimate the beneficial effects of HQD.

It is well established that HQD effectively improves the pathological symptoms of colitis such as weight loss, diarrhoea, hematochezia, and shortened colon, consistent with the efficacy of clinical medicine SASP. In addition, H&E staining showed an increase in inflammatory cells infiltration in the colon of colitis mice, caused by the activation of chemokines and the recruitment of immune cells to sites of inflammation, being improved after being treated with SASP and HQD. Notably, SASP and HQD reduced the DAI score, a reliable measure of disease severity, and repaired colon mucosal ulcers in colitis mice. WBC recruitment is an early stage linking systemic and tissue inflammation, and the increase of WBC indicated that inflammation appeared in mice with 3% DSS. The decrease of RBC and HGB in colitis mice could be due to hematochezia. However, HQD reduced the number of WBC and restored the number of RBC and the content of HGB, especially the middle-dose (500 mg/kg) and the high-dose (1000 mg/kg) of HQD. Explicitly, the data confirmed that HQD ameliorated the inflammatory response in the UC model mice.

Previous studies have shown that intestinal inflammation is frequently accompanied by imbalanced microbiota (Larabi et al.

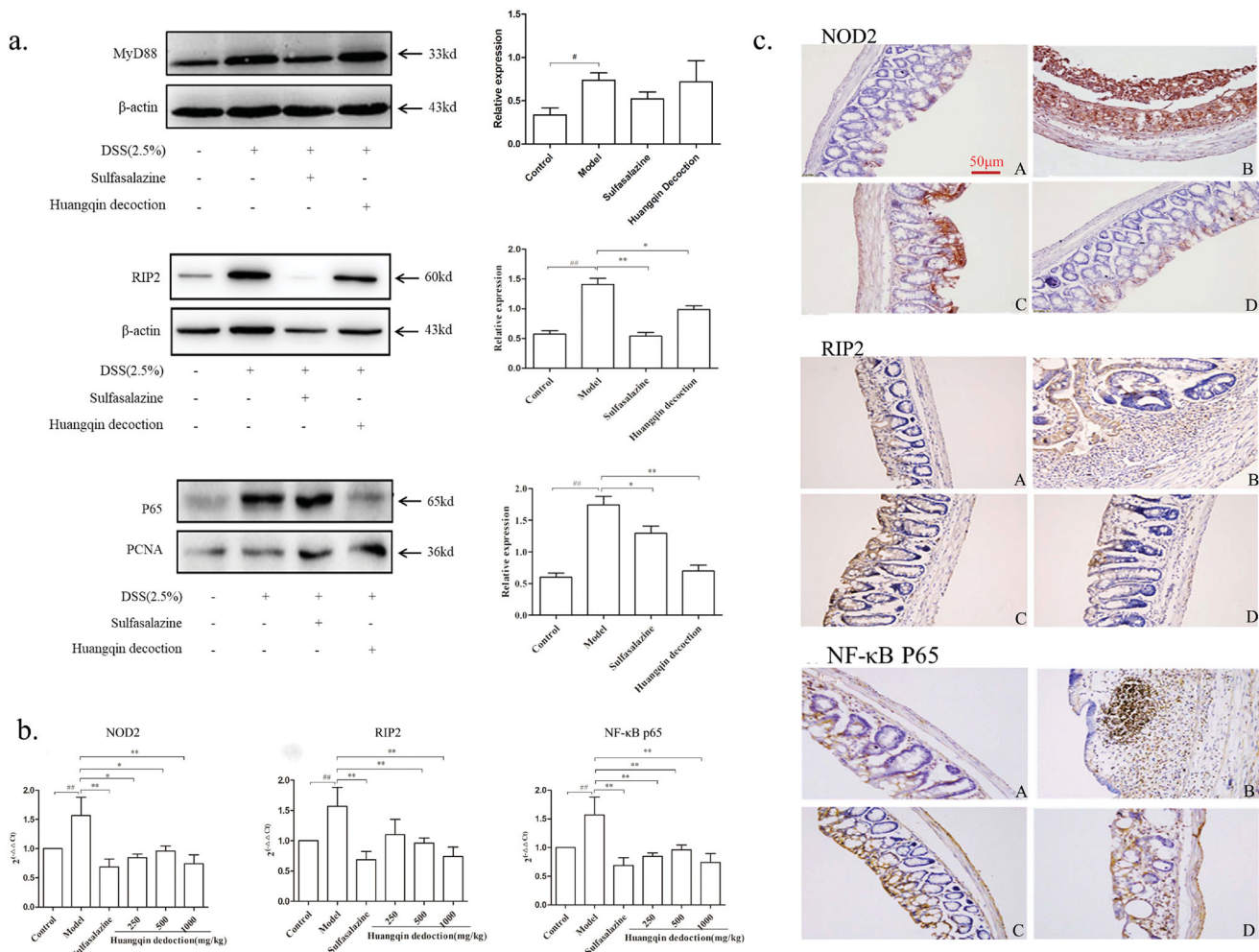


Figure 6. Effects of HQD on NOD2-dependent pathway. (a) The proteins of MyD88, RIP2, and P65 in colitis mice by western blot. The expression was normalized to that of β -actin and proliferating cell nuclear antigen (PCNA). (b) Impact of HQD on the mRNA expression of NOD2, RIP2, and NF- κ B p65 in colon samples isolated from mice ($n = 6$ per group). The expression was normalized to that of *Gapdh*. (c) Impact of HQD on the expression of proteins in the NOD2 signalling pathway in DSS-induced colitis in mice, as determined by IHC (A, Control; B, model; C, sulfasalazine; D, HQD. Magnification $\times 200$). Scale bar: 50 μ m. Data are expressed as the means \pm SD of three independent experiments. * $p < 0.01$, ** $p < 0.001$ versus DSS-treated group; # $p < 0.05$, ## $p < 0.01$ model versus control.

2020). Its components or metabolites activate the PRRs of intestinal epithelial cells and release inflammatory factors, destroying the intestinal barrier and further aggravating intestinal inflammation (Sina et al. 2018). *16S rDNA* results showed that HQD increased the OUT number and microbiota richness, consistent with the previous study (Li et al. 2019). Cluster analysis results also implied that the HQD regulated the intestinal flora and restored the diversity of intestinal flora in mice with colitis. Moreover, the data of relative abundance analysis of intestinal flora at phylum, class, and family level showed that HQD regulated intestinal flora of colitis mice, especially on reducing *Deferribacteres*, *Deferribacteraceae*, and *Alcaligenaceae*, the pathogenic bacteria. *Deferribacteres* contain the mucin-degrading *Mucispirillum* species, which can damage the integrity of the mucosal barrier. Studies have confirmed that the imbalance of intestinal flora led to conditional pathogenic bacteria invading intestinal mucosa. RegIII γ , an important bacteriostatic factor in the innate immune system, is expressed in large quantities after intestinal injury and played a role in enhancing the innate immune defence in the early stage of inflammation. The expression of RegIII γ protein raised with the increase of bacterial infiltration and inflammation. Thus, RegIII γ is used as an essential indicator of tissue injury, especially bacterial infiltration. In this

study, the intestinal contents and bacteria of colitis mice directly contacted the intestinal epithelial cells due to the destruction of the epithelial barrier caused by DSS, which stimulated the up-regulation of RegIII γ expression. FISH and FCM analysis results showed that the colonic bacterial infiltration and the RegIII γ expression of intestinal epithelial cells decreased in colitis mice after treatment with SASP and HQD, which indirectly reflected the protective effect of HQD on the intestinal barrier.

In addition, PAMPs, mainly derived from the intestinal flora of colitis mice, promoted the activation of PRRs in intestinal epithelial cells. LPS (a component of the outer wall of Gram-negative bacteria), flagellin (a granular protein that makes up the flagellar fibres of bacteria), and MDP (a smallest structural unit with adjuvant immune activity in the cytoskeleton of *Mycobacterium*) are ligands of TLR4, TLR5, and NOD2, respectively. It has been confirmed that the activation of PRRs (TLR4, TLR5, and NOD2) led to the aggravation of inflammation in colitis mice. Our data showed that the TLR4, TLR5, and NOD2 protein expression increased in the colon of colitis mice, which were decreased significantly after the intervention of HQD. The study further detected the changes of TLR4/TLR5 shared downstream pathway protein MyD88 and NOD2 downstream pathway protein RIP2. Moreover, the results showed that HQD (1000 mg/

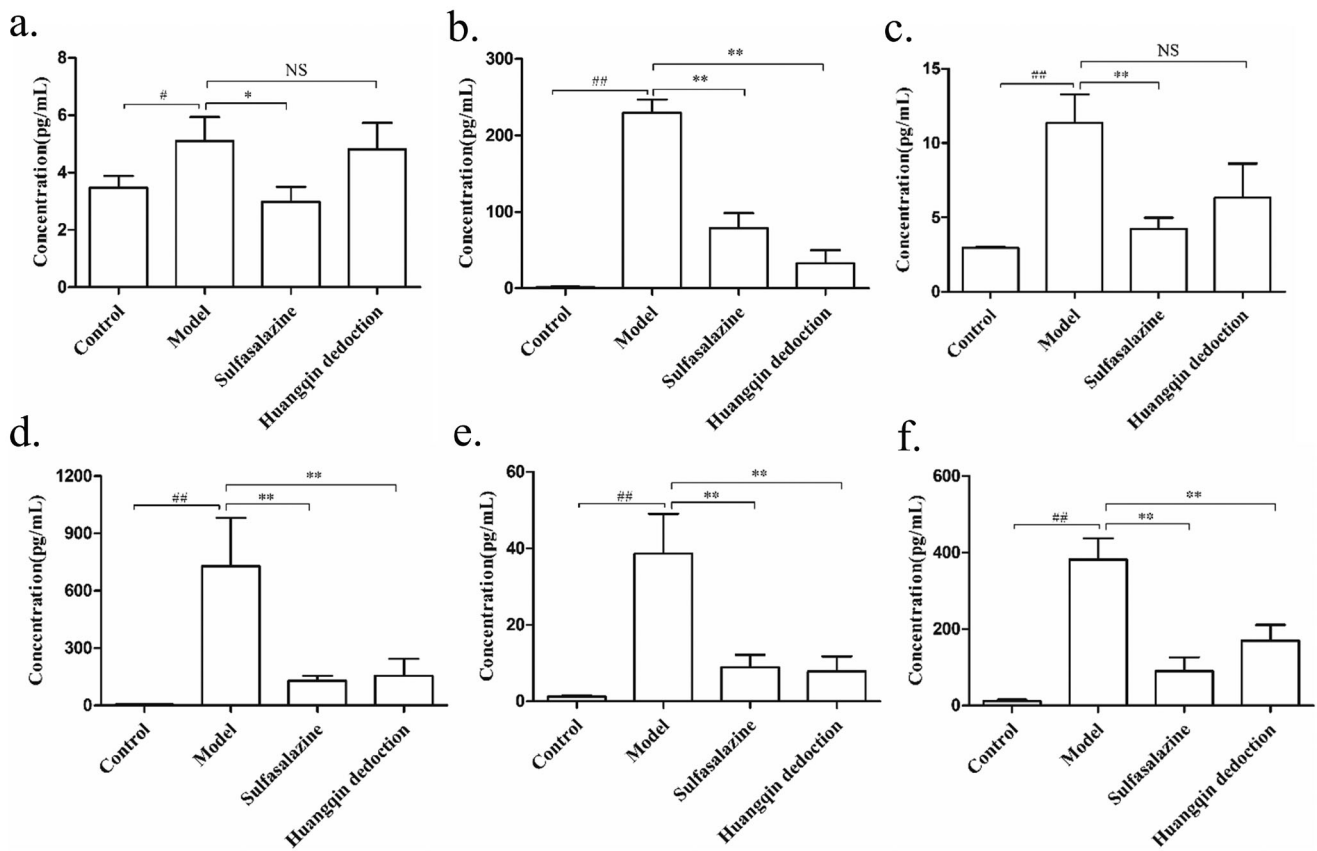


Figure 7. Effects of HQD on cytokines in the colon of DSS-induced colitis mice. Sulfasalazine and HQD, especially the medium and high doses of HQD, inhibited the release of inflammatory mediators ($n = 8$ per group): (a) IL-1 β ; (b) IL-17; (c) MCP-1; (d) TNF- α ; (e) IFN- γ ; (f) IL-6. # $p < 0.05$, ## $p < 0.01$ model versus control; * $p < 0.05$, ** $p < 0.01$ model versus HQD-treated group.

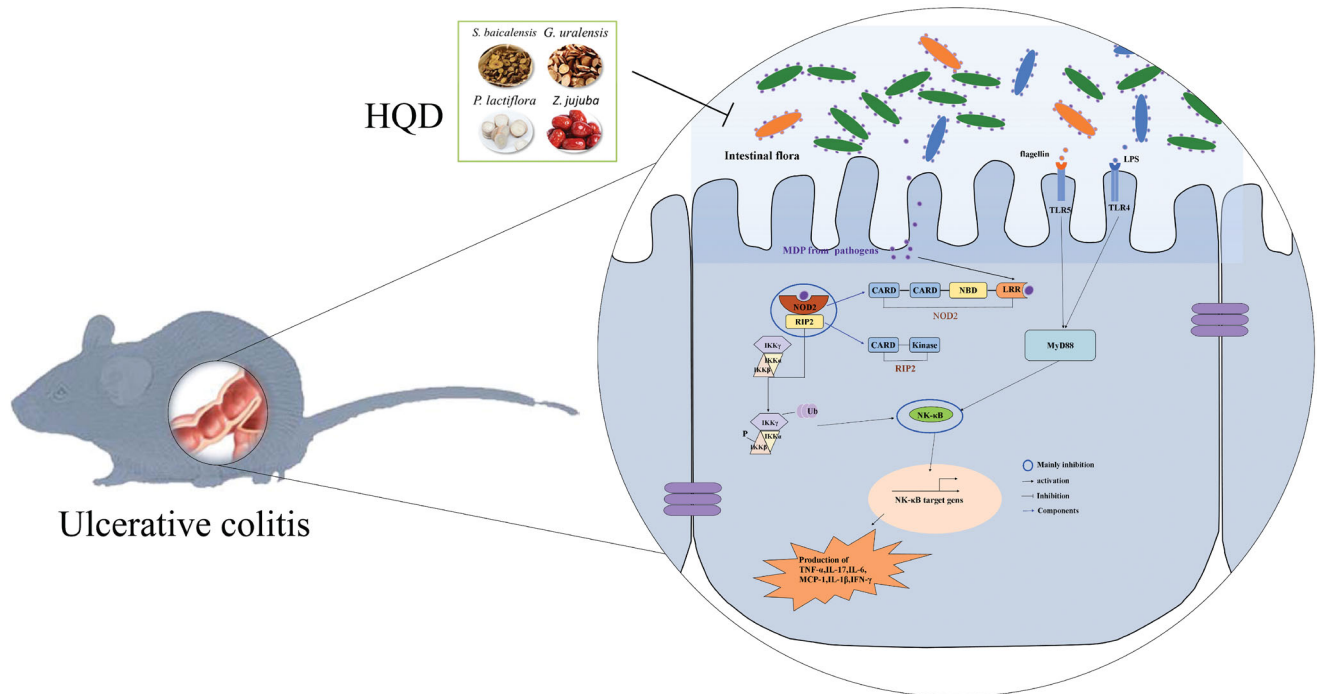


Figure 8. The mechanism of HQD (1000 mg/kg) regulates the intestinal flora of colitis mice, which may be closely characterized as inhibiting the activation of the NOD2-dependent pathway. MDP: muramyl dipeptide; NOD2: nucleotide-binding oligomerization domain 2; RIP2: receptor-interacting protein-2; NF- κ B: nuclear factor kappa-B.

kg) significantly inhibited the expression of RIP2 protein but had little effect on the expression of MyD88 protein, which was consistent with a previous study (Wang et al. 2016). Thus, we further studied the NOD2/NF- κ B signalling pathway.

As demonstrated by our data, imbalance of intestinal flora leads to the binding of PAMPs in the intestinal lumen to the PRRs of intestinal epithelial cells, further activating the PRRs-mediated pathway and exacerbates inflammation. It is known that NOD2 recognizes MDP, a product that exists in almost all bacteria, which can sense the invasion of bacteria and then activated the downstream signalling molecule RIP2. RIP2 interacted with the tumour necrosis receptor family and transcription factors activated by the NF- κ B pathway and mitogen-activated protein kinase (MAPK) pathway (Abbott et al. 2007). NF- κ B was transferred from the cytoplasm to the nucleus and bound to the promoter region of target genes, resulting in the transcription of genes encoding pro-inflammatory mediators and led to a cascade of inflammatory reactions and macrophages' recruitment the site with inflammation (Windheim et al. 2007). Hence, the activation of the NF- κ B signalling pathway is a pivotal contributor to the damage or even failure of the body tissue. NF- κ B, existing in the form of a heterodimer, consists of two subunits, p50 and p65 (Panday et al. 2016). The p65 subunit is a main pro-inflammatory subunit whose activation plays a vital role in the pathogenesis of IBD. Many IBD-associated pro-inflammatory cytokines have NF- κ B-binding sites in their promoter regions (Qian et al. 2016; Speranskii et al. 2016). Furthermore, HQD inhibited the mRNA expression of NOD2, Rip2, and NF- κ B p65, especially the high-dose HQD group (1000 mg/kg). As shown in the results of IHC, the group treated with HQD (1000 mg/kg) showed even better suppression of NOD2, RIP2, and NF- κ B p65 (Figure 8) than that treated with SASP. The increased intestinal pro-inflammatory cytokines in IBD mice further destroyed the intestinal barrier and aggravated the inflammatory response. The inflammatory cytokines (including IL-1 β , IL-17, MCP-1, TNF- α , IFN- γ , IL-6) increased in the colon and promoted the initial UC development stages (Lin et al. 2016; Liu et al. 2016), which were improved after being treated with SASP and HQD.

Conclusions

This study showed that HQD (1000 mg/kg) positively affects the imbalance of intestinal flora in colitis mice, which may be characterized as inhibiting the NOD2-dependent pathway. These results indicate that HQD might be a potential treatment for UC.

Disclosure statement

The authors declare that there are no conflicts of interest associated with this publication.

Funding

This study was supported by the National Natural Science Foundation of China [Grant nos. 81673668 and 81703785]; Natural Science Foundation of Guangdong Province (Grant no. 2018A030313447); and the Young Talents Project of Guangzhou University of Chinese Medicine [Grant no. qnyc20190104].

References

- Abbott DW, Yang Y, Hutti JE, Madhavarapu S, Kelliher MA, Cantley LC. 2007. Coordinated regulation of Toll-like receptor and NOD2 signaling by K63-linked polyubiquitin chains. *Mol Cell Biol.* 27(17): 6012–6025.
- Cooper HS, Murthy SN, Shah RS, Sedergran DJ. 1993. Clinicopathologic study of dextran sulfate sodium experimental murine colitis. *Lab Invest.* 69(2):238–249.
- Geremia A, Biancheri P, Allan P, Corazza GR, Di Sabatino A. 2014. Innate and adaptive immunity in inflammatory bowel disease. *Autoimmun Rev.* 13(1):3–10.
- Germain A, Gueant RM, Chamailard M, Allen PB, Bresler L, Gueant JL, Peyrin-Biroulet L. 2016. NOD2 gene variant is a risk factor for postoperative complications in patients with Crohn's disease: a genetic association study. *Surgery.* 160(1):74–80.
- Huang S, Fu Y, Xu B, Liu C, Wang Q, Luo S, Nong F, Wang X, Huang S, Chen J, et al. 2020. Wogonoside alleviates colitis by improving intestinal epithelial barrier function via the MLCK/pMLC2 pathway. *Phytomedicine.* 68:153179.
- Larabi A, Barnich N, Nguyen H. 2020. New insights into the interplay between autophagy, gut microbiota and inflammatory responses in IBD. *Autophagy.* 16(1):38–51.
- Li MY, Luo HJ, Wu X, Liu YH, Gan YX, Xu N, Zhang YM, Zhang SH, Zhou CL, Su ZR, et al. 2019. Anti-inflammatory effects of Huangqin decoction on dextran sulfate sodium-induced ulcerative colitis in mice through regulation of the gut microbiota and suppression of the Ras-PI3K-Akt-HIF-1 α and NF- κ B pathways. *Front Pharmacol.* 10:1552.
- Lin AN, Li YQ, Zhong MX, Liu J, Dai Q, Zhu W, Zhang YL. 2016. Expressions of inflammatory cytokines in intestinal mucosa and their prognostic value in patients with ulcerative colitis. *Nan Fang Yi Ke Da Xue Xue Bao.* 36:1712–1717.
- Liu QL, Huang L, Zhao QJ, Li Q, He Z. 2016. Relationship between serum interleukin-17 level and inflammatory bowel disease. *J Biol Regul Homeost Agents.* 30(1):181–188.
- Luo S, Deng XL, Liu Q, Pan ZF, Zhao ZX, Zhou L, Luo X. 2018. Emodin ameliorates ulcerative colitis by the flagellin-TLR5 dependent pathway in mice. *Int Immunopharmacol.* 59:269–275.
- Ning Y, Xing Y, Tian M, Bai WX, Zhang YY. 2014. Research progress of Huangqin decoction. *Chinese J Inform Trad Chinese Med.* 4:188–190 (Chinese).
- Nishida A, Inoue R, Inatomi O, Bamba S, Naito Y, Andoh A. 2018. Gut microbiota in the pathogenesis of inflammatory bowel disease. *Clin J Gastroenterol.* 11(1):1–10.
- Panday A, Inda ME, Bagam P, Sahoo MK, Osorio D, Batra S. 2016. Transcription factor NF- κ B: an update on intervention strategies. *Arch Immunol Ther Exp (Warsz).* 64(6):463–483.
- Qian J, Zhao W, Miao X, Li L, Zhang D. 2016. Sam68 modulates apoptosis of intestinal epithelial cells via mediating NF- κ B activation in ulcerative colitis. *Mol Immunol.* 75:48–59.
- Sina C, Kemper C, Derer S. 2018. The intestinal complement system in inflammatory bowel disease: shaping intestinal barrier function. *Semin Immunol.* 37:66–73.
- Speranskii AI, Kostyuk SV, Kalashnikova EA, Veiko NN. 2016. [Enrichment of extracellular DNA from the cultivation medium of human peripheral blood mononuclears with genomic CpG rich fragments results in increased cell production of IL-6 and TNF- α via activation of the NF- κ B signaling pathway]. *Biomed Khim.* 62(3):331–340.
- Ungaro R, Mehandru S, Allen PB, Peyrin-Biroulet L, Colombel JF. 2017. Ulcerative colitis. *Lancet.* 389(10080):1756–1770.
- Wan LF. 2020. Research progress of Jingfang Huangqin decoction. *Chinese Med Modern Distance Edu China.* 18:191–194 (Chinese).
- Wang C, Li Q, Ren J. 2019. Microbiota-immune interaction in the pathogenesis of gut-derived infection. *Front Immunol.* 10:1873.
- Wang DF, Wang YL, Wang YW, Guo SS, Zhuang SX, Xu HY, Li T, Yang WP. 2016. Study on the regulatory effect of Huangqin decoction on TLR4/MyD88 pathway in ulcerative colitis rats. *Acta Pharm Sin.* 51: 1558–1563.
- Wang JP, Dong LN, Wang M, Guo J, Zhao YQ. 2019. MiR-146a regulates the development of ulcerative colitis via mediating the TLR4/MyD88/NF- κ B signaling pathway. *Eur Rev Med Pharmacol Sci.* 23(5): 2151–2157.
- Weingarden AR, Vaughn BP. 2017. Intestinal microbiota, fecal microbiota transplantation, and inflammatory bowel disease. *Gut Microbes.* 8(3):238–252.

- Windheim M, Lang C, Peggie M, Plater LA, Cohen P. 2007. Molecular mechanisms involved in the regulation of cytokine production by muramyl dipeptide. *Biochem J.* 404(2):179–190.
- Xi JS. 2006. Clinical study of Huangqin decoction in treating ulcerative colitis. Beijing: Beijing University Chinese Medicine. Available from: <https://cdmd.cnki.com.cn/Article/CDMD-10026-2006085735.htm> (Chinese)
- Yang Y, Chen G, Yang Q, Ye J, Cai X, Tsering P, Cheng X, Hu C, Zhang S, Cao P. 2017. Gut microbiota drives the attenuation of dextran sulphate sodium-induced colitis by Huangqin decoction. *Oncotarget.* 8(30):48863–48874.
- Zhang X, Zhang S, He RB, Shan Y, Chen DC. 2017. Intestinal microbial barrier function and virulence of pathogenic. *Prog in Mod Biomed.* 17: 6186–6190.
- Zhang Y, Shen N. 2018. The variation characteristics of intestinal flora in patients with ulcerative colitis. *Hebei Med J.* 40:1054–1057.
- Zou Y, Lin J, Li W, Wu Z, He Z, Huang G, Wang J, Ye C, Cheng X, Ding C, et al. 2016. Huangqin-tang ameliorates dextran sodium sulphate-induced colitis by regulating intestinal epithelial cell homeostasis, inflammation and immune response. *Sci Rep.* 6:39299.